

A&A 401, 129–140 (2003)
DOI: 10.1051/0004-6361:20021863
© ESO 2003

**Astronomy
&
Astrophysics**

On the difference between the short and long gamma-ray bursts

L. G. Balázs¹, Z. Bagoly², I. Horváth³, A. Mészáros⁴, and P. Mészáros⁵

¹ Konkoly Observatory, Budapest, Box 67, 1525, Hungary

² Laboratory for Information Technology, Eötvös University, Budapest, Pázmány Péter sétány 1/A, 1117, Hungary
e-mail: bagoly@ludens.elte.hu

³ Dept. of Physics, Bolyai Military University, Budapest, Box 12, 1456, Hungary
e-mail: hoi@bjkmf.hu

⁴ Astronomical Institute of the Charles University, 180 00 Prague 8, V Holešovičkách 2, Czech Republic
e-mail: meszaros@mbbox.cesnet.cz

⁵ Dept. of Astronomy & Astrophysics, Pennsylvania State University, 525 Davey Lab
e-mail: nnp@astro.psu.edu

Received 29 August 2002 / Accepted 16 December 2002

Abstract. We argue that the distributions of both the intrinsic fluence and the intrinsic duration of the γ -ray emission in gamma-ray bursts from the BATSE sample are well represented by log-normal distributions, in which the intrinsic dispersion is much larger than the cosmological time dilatation and redshift effects. We perform separate bivariate log-normal distribution fits to the BATSE short and long burst samples. The bivariate log-normal behaviour results in an ellipsoidal distribution, whose major axis determines an overall statistical relation between the fluence and the duration. We show that this fit provides evidence for a power-law dependence between the fluence and the duration, with a statistically significant different index for the long and short groups. We discuss possible biases, which might affect this result, and argue that the effect is probably real. This may provide a potentially useful constraint for models of long and short bursts.

Key words. gamma-rays: bursts – methods: statistical – methods: data analysis

1. Introduction

The simplest grouping of gamma-ray bursts (GRBs), which is still lacking a clear physical interpretation, is given by their well-known bimodal duration distribution. This divides bursts into long ($T \gtrsim 2$ s) and short ($T \lesssim 2$ s) duration groups (Kouveliotou et al. 1993), defined through some specific duration definition such as T_{90} , T_{50} or similar. The bursts measured with the BATSE instrument on the Compton Gamma-Ray Observatory are usually characterized by 9 observational quantities, i.e. 2 durations, 4 fluences and 3 peak fluxes (Meegan et al. 1996; Paciesas et al. 1999; Meegan et al. 2001). In a previous paper (Bagoly et al. 1998) we used the principal components analysis (PCA) technique to show that these 9 quantities can be reduced to only two significant independent variables, or principal components (PCs). These PCs can be interpreted as principal vectors, which are made up of some subset of the original observational quantities. The most important PC is made up essentially by the durations and the fluences, while the second, weaker PC is largely made up of the peak fluxes. This simple observational fact, that the dominant principal component consists mainly of the durations and

the fluences, may be of consequence for the physical modeling of the burst mechanism. In this paper we investigate in greater depth the nature of this principal component decomposition, and, in particular, we analyze quantitatively the relationship between the fluences and durations implied by the first PC. In our previous PCA treatment of the BATSE Catalog (Paciesas et al. 1999) we used logarithmic variables, since these are useful for dealing with the wide dynamic ranges involved. Since the logarithms of the durations and the fluences can be explained by only one quantity (the first PC), one might suspect the existence of only one physical variable responsible for both of these observed quantities. The PCA assumes a linear relationship between the observed quantities and the PC variables. The fact that the logarithmic durations and fluences can be adequately described by only one PC implies a proportionality between them and, consequently, a power law relation between the observed durations and fluences. We analyze the distribution of the observed fluences and durations of the long and the short bursts, and we present arguments indicating that the intrinsic durations and fluences are well represented by log-normal distributions. The implied bivariate log-normal distribution represents an ellipsoid in these two variables, whose major axis inclinations are statistically different for the long and the short bursts. An analysis of the possible biases and complications is

Send offprint requests to: L. G. Balázs,
e-mail: balazs@konkoly.hu

made, leading to the conclusion that the relationship between the durations and fluences appears to be intrinsic, and may thus be related to the physical properties of the sources themselves. We calculate the exponent in the power-laws for the two types of bursts, and find that for the short bursts the total emitted energy is weakly coupled to the intrinsic duration, while for the long ones the fluences are roughly proportional to the intrinsic durations. The possible implications for GRB models are briefly discussed.

The paper is organized as follows. Section 2 (Sect. 3) provides classical χ^2 fitting of the measured durations (fluences) – separately for the short and long GRBs. The purposes of these two Sections is to show that – separately for the two subgroups – both the intrinsic durations and also the total emitted energies are distributed log-normally. Using these results in Sect. 4 a simultaneous fitting of the fluences and the measured durations are done by the superposition of two bivariate log-normal distributions. The purpose of this section is to find the power-law connections between the fluences and durations – separately for the two subgroups. Because the observational biases may play an essential role in these results the biases are studied in this section, too. Section 5 discusses and summarizes the results of article. In the Appendix some technical calculations are presented.

2. Analysis of the duration distribution

Our GRB sample is selected from the Current BATSE Gamma-Ray Burst Catalog according to two criteria, namely, that they have both measured T_{90} durations and fluences (for the definition of these quantities see Meegan et al. 2001, henceforth referred to as the Catalog). The Catalog in its final version lists 2041 bursts for which a value of T_{90} is given. The fluences are given in four different energy channels, F_1, F_2, F_3, F_4 , whose energy bands correspond to [25, 50] keV, [50, 100] keV, [100, 300] keV and >300 keV. The “total” fluence is defined as $F_{\text{tot}} = F_1 + F_2 + F_3 + F_4$. We restrict our sample to include only those GRBs, which have $F_i > 0$ values in the first three channels; i.e. F_1, F_2, F_3 are given. Concerning the fourth channel, whose energy band is >300 keV, if we had required $F_4 > 0$ as well, this would have reduced the number of eligible GRBs by $\simeq 20\%$. Hence, we decided to accept also these bursts with $F_4 = 0$, rather than deleting them from the sample. (With this choice we also keep in the sample the no-high-energy (NHE) subgroup defined by Pendleton et al. 1997.) Our choice of $F \equiv F_{\text{tot}}$, instead of some other quantity as the main variable, is motivated by two arguments. First, as discussed in Bagoly et al. (1998), F_{tot} is the main constituent of one of the two PCs which represent the data embodied in the BATSE Catalog, and hence it can be considered as a primary quantity, rather than some other combination or subset of its constituents. Second, Petrosian and collaborators in a series of articles (Efron & Petrosian 1992; Petrosian & Lee 1996; Lee & Petrosian 1996, 1997) have also argued for the use of the fluence as the primary quantity instead of, e.g., the peak flux. Using such defined F_{tot} , from the sample only such GRBs are deleted, which have no measured F_{tot} . Because also the peak fluxes are needed, too, we are left with $N = 1929$ GRBs, all

of which have defined T_{90} and F_{tot} , as well as peak fluxes P_{256} on the 256 ms trigger scale. If the peak flux P_{64} on the 64 ms trigger scales is needed, then the sample contains $N = 1972$ GRBs. These are the samples studied in this article.

The distribution of the logarithm of the observed T_{90} displays two prominent peaks¹, which is interpreted as reflecting the existence of two groups of GRBs (Kouveliotou et al. 1993; Norris et al. 2001). This bimodal distribution can be well fitted by the sum of two Gaussian distributions (Horváth 1998) indicating that both the long and the short bursts are individually well fitted by pure Gaussian distributions in the logarithmic durations. The fact that the distribution of the BATSE T_{90} quantities within a group is log-normal is of interest, since we can show that this property may be extended to the *intrinsic* durations as well. Let us denote the observed duration of a GRB with T_{90} (which may be subject to cosmological time dilatation), and denote with t_{90} the duration which would be measured by a comoving observer, i.e. the intrinsic duration. One has

$$T_{90} = t_{90}f(z), \quad (1)$$

where z is the redshift, and $f(z)$ measures the time dilatation. For the concrete form of $f(z)$ one can take $f(z) = (1+z)^k$, where $k = 1$ or $k = 0.6$, depending on whether energy stretching is included or not (Fenimore & Bloom 1995; Mészáros & Mészáros 1996). If energy stretching is included, for different photon frequencies ν the t_{90} depends on these frequencies as $t_{90}(\nu) = t_{90}(\nu_0)(\nu/\nu_0)^{-0.4} \propto \nu^{-0.4}$, where ν_0 is an arbitrary frequency in the measured range (i.e. for higher frequencies the intrinsic duration is shorter). The observed duration at ν is simply $(1+z)$ times the intrinsic duration at $\nu \times (1+z)$. Thus, $T_{90}(\nu) = t_{90}(\nu(1+z))(1+z) = t_{90}(\nu_0)(\nu(1+z)/\nu_0)^{-0.4}(1+z) = t_{90}(\nu)(1+z)^{0.6}$. Hence, when stretching is included, $f(z) = (1+z)^{0.6}$ is used. Taking the logarithms of both sides of Eq. (1) one obtains the logarithmic duration as a sum of two independent stochastic variables. According to a mathematical theorem of Cramér (Cramér 1937; Rényi 1962), if a variable ζ – which has a Gaussian distribution – is given by the sum of two independent variables, e.g. $\zeta = \xi + \eta$, then both ξ and η have Gaussian distributions. (In practical cases, however, this holds, of course, only if the variances of ξ and η are comparable. If the variance of, say, ξ is much smaller than the variance of η , then both the variables ζ and η may have a normal distribution – but nothing can be said about the distribution of ξ . It can, but also need not be Gaussian.)

Therefore, the Gaussian distribution of $\log T_{90}$ – confirmed for the long and short groups separately (Horváth 1998) – implies that the same type of distribution exists for the variables $\log t_{90}$ and $\log f(z)$. However, unless the space-time geometry has a very particular structure, the distribution of $\log f(z)$ cannot be Gaussian. This means that the Gaussian nature of the distribution of $\log T_{90}$ must be dominated by the distribution

¹ There is also an evidence for the existence of a third intermediate subgroup as part of the long duration group (Horváth 1998; Mukherjee et al. 1998; Hakkila et al. 2000a,c; Balastegui et al. 2001; Horváth 2002), which shows a distinct sky angular distribution (Mészáros et al. 2000a,b; Litvin et al. 2001). We do not deal with this third group here.

of $\log t_{90}$ alone, and therefore the latter must then necessarily have a Gaussian distribution. In other words, the variance of $f(z)$ must be much smaller than the variance of $\log t_{90}$. This must hold for both duration groups separately. This also implies that the cosmological time dilatation should not affect significantly the observed distribution of T_{90} , which therefore is not expected to differ statistically from that of t_{90} . We note that several other authors (Wijers & Paczyński 1994; Norris et al. 1994; Norris et al. 1995) have already suggested that the distribution of T_{90} reflects predominantly the distribution of t_{90} . Nevertheless, our argumentation based on the mathematical Cramér theorem is new.

One can check the above statement quantitatively by calculating the standard deviation of $f(z)$, using the available observed redshifts of GRB optical afterglows. The number of the latter is, however, relatively modest, and, in addition, so far they have been obtained only for long bursts. There are currently upwards of 21 GRBs with well-known redshifts (Greiner 2002). The calculated standard deviation is $\sigma_{\log f(z)} = 0.17$, assuming $\log f(z) = \log(1+z)$. Comparing the variance $\sigma_{\log f(z)}^2$ with that of the group of long burst durations which gives $\sigma_{\log T_{90}} = 0.5$, one infers that the variance of $\log f(z)$, or of $\log(1+z)$, can explain maximally only about $(0.17/0.50)^2 \simeq 12\%$ of the total variance of the logarithmic durations. (If $f(z) = (1+z)^{0.6}$, then the variance of $\log f(z)$ can only explain an even smaller amount, because $\sigma_{\log f(z)} = 0.6 \times 0.17$.) This comparison supports the conclusion obtained by applying Cramér's theorem to the long duration group. For the short duration group, since this does not so far have measured redshifts, one can rely only on the theorem itself.

3. Analysis of the fluence distribution

The observed total fluence F_{tot} can be expressed as

$$F_{\text{tot}} = \frac{(1+z)E_{\text{tot}}}{4\pi d_1^2(z)} = c(z)E_{\text{tot}}. \quad (2)$$

Here E_{tot} is the total emitted energy of the GRB at the source in ergs, the total fluence has dimension of erg/cm^2 , and $d_1(z)$ is the luminosity distance corresponding to z for which analytical expressions exist in any given Friedmann model (Weinberg 1972; Peebles 1993). (We note that the considerations in this paper are valid for any Friedmann model. Note also that the usual relation between the luminosity and flux is given by a similar equation without the extra $(1+z)$ term in the numerator. Here this extra term is needed because both the left-hand-side is integrated over the observer-frame time and the right-hand-side is integrated over the time at the source (Mészáros & Mészáros 1995).)

Assuming as the null hypothesis that the $\log F_{\text{tot}}$ of the short bursts has a Gaussian distribution, for the sample of 447 bursts with $T_{90} < 2$ s, a χ^2 test with 26 degrees of freedom gives an excellent fit with $\chi^2 = 20.17$. Accepting the hypothesis of a Gaussian distribution within this group, one can apply again Cramér's theorem similarly to what was done for the logarithm of durations. This leads to the conclusion that either both the distribution of $\log c(z)$ and the distribution of $\log E_{\text{tot}}$

are Gaussian ones, or else the variance of one of these quantities is negligible compared to the other, which then must be mainly responsible for the Gaussian behaviour. Because $\log c(z)$ hardly can have a log-normal distribution, the second possibility seems to be the situation. In any case, one may conclude that the intrinsic fluence (i.e. the total emitted energy) should be distributed log-normally.

In the case of the long bursts, a fit to a Gaussian distribution of logarithmic fluences does not give a significance level, which is as convincing as for the short duration group. For the 1482 GRBs with $T_{90} > 2$ s a χ^2 test on $\log F_{\text{tot}}$ with 22 degrees of freedom gives a fit with $\chi^2 = 35.12$. Therefore, in this case the χ^2 test casts some doubt on normality but only with a relatively high error probability of 3.5% for rejecting a Gaussian distribution (Trumpler & Weaver 1953; Kendall & Stuart 1976; Press et al. 1992). This circumstance prevent us from applying Cramér's theorem directly in the same way as we did with the short duration group. Calculating the variance of $\log c(z)$ for the GRBs with known 21 redshifts (Greiner 2002) one obtains $\sigma_{\log c(z)} = 0.43$. For the GRBs of long duration, however, one obtains $\sigma_{\log F_{\text{tot}}} = 0.66$. The ratio of these variances equals $(0.43^2/0.66^2) \simeq 42\%$, i.e. more than half of the variance of F_{tot} is not explained by the variance of $c(z)$. (If one takes into account the energy stretching even a larger fraction remains unexplained.) In other words, a significant fraction of the total variance of F_{tot} has to be intrinsic. It is worth mentioning that the unexplained part of the variance of F_{tot} corresponds nicely to the value obtained in Sect. 4 making use the EM algorithm.

Despite these difficulties, there is a substantial reason to argue that the intrinsic distribution of total emitted energies is distributed log-normally for the long subgroup, too.

The Gaussian behaviour of $\log c(z)$ can almost certainly be excluded. One can do this on the basis of the current observed distribution of redshifts (Greiner 2002), or on the basis of fits of the number vs. peak flux distributions (Fenimore & Bloom 1995; Ulmer & Wijers 1995; Horváth et al. 1996; Reichart & Mészáros 1997). In such fits, using a number density $n(z) \propto (1+z)^D$ with $D \simeq (3-5)$, one finds no evidence for the stopping of this increase with increasing z (up to $z \simeq (5-20)$). Hence, it would be contrived to deduce from this result that the distribution of $\log c(z)$ is normal. In order to do this, one would need several ad hoc assumptions. First, the increasing of number density would need to stop around some unknown high z . This was studied (Mészáros & Mészáros 1995; Horváth et al. 1996; Mészáros & Mészáros 1996), and no such effect was found. (For the sake of preciseness it must be added here that these fits were done for the whole sample of GRBs. But, because GRBs are dominated by the long ones, conclusions from these fits should hold for the long subgroup, too.) Second, even if this were the case, above this z the decrease of $n(z)$ should mimic the behavior of a log-normal distribution for $c(z)$, without any obvious justification. Third, below this z one must again have a log-normal behavior for $c(z)$, in contradiction with the various number vs. peak flux fits. Fourth, this behavior should occur for any subclass separately. Hence, the assumption of log-normal distribution of $c(z)$ appears highly improbable.

Having a highly improbable log-normal distribution of $\log c(z)$, which variance is surely not negligible, a 3.5% error probability (i.e. the probability that we reject the hypothesis of normality but it is still true) from the goodness-of-fit is still remarkable. One may argue that, if the distribution of the total emitted energy were not distributed log-normally, then the two non-normal distributions together would give a fully wrong χ^2 fit for $\log F_{\text{tot}}$; under this condition even the 3.5% probability would not be reachable. Of course, this argumentation is more or less heuristic, and – as the conclusion – one cannot say that the log-normal distribution of E_{tot} is confirmed similarly unambiguously in both subgroups. In the case of long subgroup questions still remain, and they will still be discussed (end of Sect. 4.3). It is worth mentioning the rise times, fall times, *FWHM*, pulse amplitudes and areas were measured and the frequency distributions are consistent with log-normal distributions (McBreen et al. 2001; Quilligan et al. 2002).

In addition, even in the case of short GRBs the situation is not so clear yet. The argument based on the Cramér theorem for the short GRBs should also be taken with some caution. As shown in Bagoly et al. (1998), the stochastic variable corresponding to the duration is independent from that of the peak flux. This means that a fixed level of detection, given by the peak fluxes, does not have significant influence on the shape of the detected distribution of the durations (Efron & Petrosian 1992; Wijers & Paczyński 1994; Norris et al. 1994, 1995; Petrosian & Lee 1996; Lee & Petrosian 1996, 1997). In the case of the fluences, however, a detection threshold in the peak fluxes induces a bias on the true distribution, since fluences and durations are stochastically not independent. Therefore, the log-normal distribution recognized from the data does not necessarily imply the same behaviour for the true distribution of fluences occurring at the detector. In other words, observational biases may have important roles; in addition, for both subgroups. A discussion of these problems can be found in a series of papers published by Petrosian and collaborators (Efron & Petrosian 1992; Petrosian & Lee 1996; Lee & Petrosian 1996, 1997; Lloyd & Petrosian 1999). In what follows, we also will study the biases together with the fitting procedures.

4. Correlation between the fluence and duration

In the previous sections we presented firm evidences that the observed distribution of the durations is basically intrinsic. We argued furthermore that a significant fraction of the variance of the fluences is also intrinsic. We proceed a step further in this section and try to demonstrate that there is a relationship between the duration and the fluence which is also intrinsic. There are two basic difficulties in searching the concrete form of this relationship (if there is any at all): first, we observe only those bursts which fulfill some triggering criteria and, second, the observed quantities are suffering from some type of bias depending on the process of detection. Several papers discuss these biases (Efron & Petrosian 1992; Lamb et al. 1993; Lee & Petrosian 1996; Petrosian & Lee 1996; Lee & Petrosian 1997; Stern et al. 1999; Paciesas et al. 1999; Hakkila et al. 2000b; Meegan et al. 2000). In the following we will address these issues in a new way.

The detection proceeds on three time scales: the input signal is analyzed on 64, 256 and 1024 ms resolution. The counts in these bins of these scales are compared with the corresponding 17 s long averaged value. There are eight detectors around the BATSE instrument. If at least one of the three peak intensities in the second brightest detector exceeds 5.5 sigma of the threshold computed from the averaged signal the burst will be detected. In case of the bursts of long duration (at least several seconds) the differences in the time scales of detection do not play an important role since the vast majority of the events were triggered on the 1024 ms scale and the detection proceeded if the peak exceeded the threshold on this time scale. In contrast, at the bursts of short duration – when T_{90} could be much shorter than the time scale of the detection – the situation could be drastically changed. Looking at the data of the BATSE the bursts of duration of $T_{90} < 2$ s are mixtures of those triggered on different time scales. Among bursts triggered on the same time scale the detection proceeds when the corresponding peak flux exceeds the threshold. In the case of bursts, which are shorter than their triggering time scale, the corresponding peak fluxes are given by the fluence itself. This has the consequence that the threshold in the peak flux means the same for the fluence, i.e. it results a horizontal cut on the fluence – duration plane and a bias in the relationship between these quantities. In order to minimize this effect we will use the peak flux on the 64 ms and 256 ms time scale in our further analysis. The BATSE had a spectral response on the detected γ radiation. It had the consequence that different measured values were assigned to bursts having the same total energy at the entrance of the detector if the incoming photons had different spectral distributions.

The duration of a GRB is only a lower limit for its intrinsic value since a certain fraction of the burst can be buried in the background noise. Therefore any relationship recognized among the observed fluence and duration is not necessarily representative for those between the corresponding intrinsic quantities. In the next paragraphs we address these issues in more details.

4.1. Effect of the detection threshold on the joint probability distribution of the fluence and duration

In the following we will study the effect of the detection threshold on the joint probability distribution of the observed fluence and duration. In order to put this effect into a quantitative basis we use the law of full probabilities (see e.g. Rényi 1962). Let $P(F_{\text{tot}}, T_{90})$ be the joint probability density of the fluence and duration. Using this theorem any of the probability densities on the right side can be written in the form of

$$P(F_{\text{tot}}, T_{90}) = \int_0^{\infty} P(F_{\text{tot}}, T_{90}|p)G(p)dp, \quad (3)$$

where p is the peak flux at any of the 64 ms, 256 ms and 1024 ms time scales, $P(F_{\text{tot}}, T_{90}|p)$ is the joint (bivariate) probability density of the fluence and duration (assuming that p is given), and $G(p)$ is the probability density of p . This means that, if there are N bursts in the sample, then

$NP(F_{\text{tot}}, T_{90}) d \log F_{\text{tot}} d \log T_{90}$ is the expected number of observed GRBs in the infinitesimal intervals $[\log F_{\text{tot}}, (\log F_{\text{tot}} + d \log F_{\text{tot}})]$ and $[\log T_{90}, (\log T_{90} + d \log T_{90})]$, respectively. Among the bursts triggered on a given time scale $G(p)$ represents an unbiased function above p_{th} , the peak flux corresponding to the detection threshold. Below this limit, however, $G(p)$ is biased by the process of detection. It inserts also a bias on the joint probability density of the observed fluence and duration. Nevertheless, the kernel $P(F_{\text{tot}}, T_{90}|p)$ represents some intrinsic relationship between these two quantities, and it is free from the bias of $G(p)$. Following our discussion given above, we use in the following the peak fluxes of the 64 ms time scale.

4.2. Intrinsic relationship between the fluence and the duration

We demonstrated in an earlier paper (Bagoly et al. 1998) that the logarithms of the peak flux and the duration represent two independent stochastic variables and the logarithmic fluence can be well approximated as the linear combination of these variables:

$$\log F_{\text{tot}} = a_1 \log T_{90} + a_2 \log p + \epsilon, \quad (4)$$

where a_1, a_2 are constants, and ϵ is a noise term (later on we will see that a_1 may depend on the duration, i.e. it is different for the bursts of short and long duration). One may confirm this statement by inspecting the tables given in the Appendix. They demonstrate convincingly that, independently of the choice of the peak flux, the standard deviation and the mean value of the duration is not changed significantly. This expression reveals that – fixing the peak intensity – the distribution of the fluences reflects basically the distribution of the durations. Since the probability density of the durations is a superposition of two Gaussian distributions, the same should hold also for the fluences. Consequently, we may assume that the joint conditional probability distribution of the fluence and duration consists of a superposition of two two-dimensional Gaussian distributions. One such distribution takes the form

$$f(x, y) dx dy = \frac{N}{2\pi\sigma_x\sigma_y\sqrt{1-r^2}} \times \exp\left[-\frac{1}{2(1-r^2)} \times \left(\frac{(x-a_x)^2}{\sigma_x^2} + \frac{(y-a_y)^2}{\sigma_y^2} - \frac{2r(x-a_x)(y-a_y)}{\sigma_x\sigma_y}\right)\right] dx dy, \quad (5)$$

where $x = \log T_{90}$, $y = \log F_{\text{tot}}$, a_x, a_y are the means, σ_x, σ_y are the dispersions, and r is the correlation coefficient (Trumpler & Weaver 1953, Chap. 1.25). In our case one needs a weighted sum of two such bivariate distributions. This means that 11 free parameters should be determined (two times 5 parameters for the both distributions; the 11th independent parameter is the weight of the, say, first subgroup). This also means that two r correlation coefficients should be obtained, which may be different for the two subgroups.

The parameters a_x, σ_x , characterizing the distribution of the duration do not depend on the peak flux, because T_{90} and p are independent stochastic variables. The only dependent parameter is a_y , the mean value of the fluence. In the case, when the r -correlation coefficient differs from zero, the semi-major

axis of the dispersion ellipse represents a linear relationship between $\log T_{90}$ and $\log F_{\text{tot}}$, with a slope of $m = \tan \alpha$, where

$$\tan 2\alpha = \frac{2r\sigma_x\sigma_y}{\sigma_x^2 - \sigma_y^2}. \quad (6)$$

This linear relationship between the logarithmic variables implies a power-law relation of form $F_{\text{tot}} = (T_{90})^m$ between the fluence and the duration, where m may be different for the two groups. Replacing the $G(p)$ probability density by the empirical distribution of the measured peak fluxes, one may write the joint probability density of the fluence and duration in the form of

$$P(F_{\text{tot}}, T_{90}) = \int_0^\infty P(F_{\text{tot}}, T_{90}|p)G(p)dp \approx \sum_{i=1}^N P(F_{\text{tot}}, T_{90}|p_i) \approx \sum_{i=1}^k b_i P(F_{\text{tot}}, T_{90}|p_i), \quad (7)$$

i.e. the integral is approximated by a sum of k separate terms (bins), in which b_i is the number of GRBs at the given bin.

The k is the number of bins at the right-hand-side, and is somewhat arbitrary. Trivially, bigger k leads to a better approximation of the integral. On the other hand, bigger k leads to the situation, when in one single bin the number of GRBs b_i is smaller. Hence, k should be small in order to get enough number of GRBs in each bin for making statistics, but not too small in order to have good approximation of the integral.

4.3. Maximum Likelihood estimation of the parameters via EM algorithm

One finds in the tables of Appendix the computed mean values and standard deviations of the logarithmic durations for the short and long bursts, respectively. These tables clearly suggest that, except for the faintest bins where we expect serious biases in the duration and fluence due to the detection close to the background, the standard deviations do not differ significantly between the bins. Dividing the sample into short and long bursts by the cut of $T_{90} < 2$ s and $T_{90} > 2$ s, we may assume that these subsamples are dominated by only one Gaussian distribution and we may compute its parameters in a simple way as given below. If the $P(F_{\text{tot}}, T_{90}|p)$ conditional probability density is a pure Gaussian one, then the Maximum Likelihood (ML) estimation of its parameters would be very simple, because they can be obtained by computing the mean values, standard deviations and the correlation between the fluence and duration. In the reality, however, this probability density is a superposition of two Gaussians one, and the simple cut at $T_{90} = 2$ s is hardly satisfactory. The proper way to estimate the free parameters is not so simple. For this reason we will use a procedure, called EM algorithm (Expectation and Maximalization), which terminates at the ML solution (Dempster et al. 1977). If we knew, which of the bursts belong to the short and long duration groups, we may add a $\{i_1, i_2\}$ two dimensional indicator variable to each GRB having the value of $\{1, 0\}$ in the case if a burst was short, and similarly $\{0, 1\}$ if it was long. The sample means of T_{90} weighted with i_1

Table 1. Number of GRBs within the 0.2 wide strata of the logarithmic 64 ms peak fluxes.

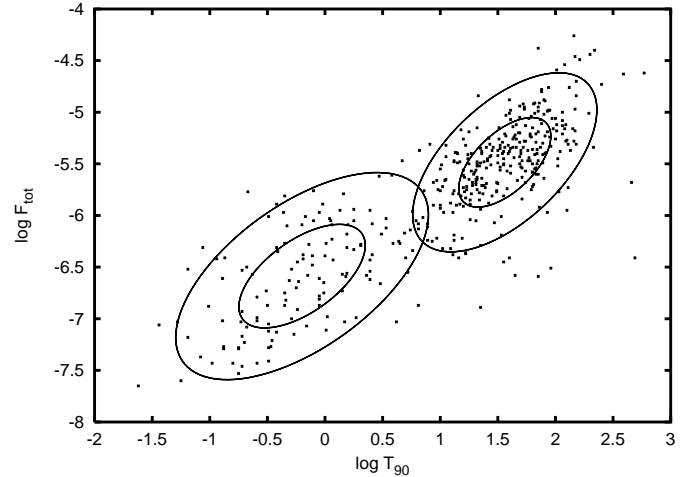
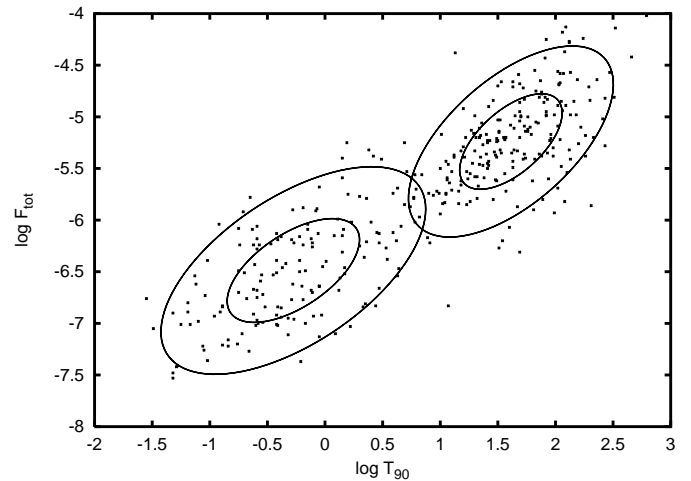
Serial No.	$\log P_{64}$	total No. of GRBs	No. of GRBs with $T_{90} < 2$ s	No. of GRBs with $T_{90} < 0.064$ s
1.	-0.6–-0.4	5	1	0
2.	-0.4–-0.2	113	5	0
3.	-0.2–0.0	385	44	1
4.	0.0–0.2	434	104	4
5.	0.2–0.4	365	126	8
6.	0.4–0.6	254	79	3
7.	0.6–0.8	166	47	2
8.	0.8–1.0	95	34	0
9.	1.0–1.2	74	22	0
10.	1.2–1.4	39	6	0
11.	1.4–1.6	19	5	0
12.	1.6–1.8	15	2	0
13.	1.8–2.0	6	1	0
14.	2.0 <	2	0	0

would give the ML estimation of a_x of the first Gaussian distribution (i.e. $a_x = \sum_{j=1}^N i_{1j}x_j / \sum_{j=1}^N i_{1j}$). The same hold for the other parameters. Weighting with i_2 would give the parameters of the second Gaussian distribution. Hence 10 parameters of the two distributions would be well calculable. The 11th parameter would also be trivially calculable, because the fraction of first subgroup should simply be $\sum_{i=1}^N i_1 / N$. Hence, if the values of the $\{i_1, i_2\}$ indicator variable were known, the ML parameters would be well calculable.

If the parameters of the two Gaussians were given, one could compute the $\{p_1, p_2\}$ membership probabilities of a burst to each of the two groups. Replacing the indicator variable by these probabilities one may calculate new parameters in the same way as was done assuming $\{i_1, i_2\}$ were given. Then one may again calculate new $\{i_1, i_2\}$, and again the new parameters. This iteration is exactly the procedure, what EM algorithm is doing. One gives an initial estimate for the parameters of the two Gaussian distributions. Then one estimates the membership probabilities (E step). Weighting with the membership probabilities one obtains the new ML estimation of the parameters (M step). Repeating these steps successively one proceeds to the ML solution of the parameter estimation (Dempster et al. 1977).

In order to fit the $[\log T_{90}, \log F_{\text{tot}}]$ data pairs with the superposition of two two-dimensional Gaussian bivariate distributions we splitted the Catalog into subsamples with respect to 64 ms peak fluxes. The strata were obtained by taking 0.2 wide strips in the logarithmic peak fluxes. Table 1 summarizes the number of GRBs within the strata. In addition, also the number of GRBs with $T_{90} < 2$ s and with $T_{90} < 0.064$ s are given there. The first one shows that, roughly, which fraction of GRBs belong to the short subgroup in the given strata, and the second one shows which fraction is maximally biased.

In the fitting procedure we omitted bins No. 1–3, being affected by selection bias, and also No. 9–14, being scarcely populated. We performed the ML fitting in the bins No. 4–8, making use the EM algorithm. Table 2 summarizes the results of the ML fitting for the short GRBs, and Table 3 for the long

**Fig. 1.** The best ML fits of the two log-Gaussian distributions for the faintest sample No. 4 with $N = 434$.**Fig. 2.** The best ML fits of the two log-Gaussian distributions for the sample No. 5 with $N = 365$.

GRBs, respectively. In Figs. 1–5 the results of fitting for bins No. 4–8 are shown. The ellipses define the 1-sigma and 2-sigma regions, respectively.

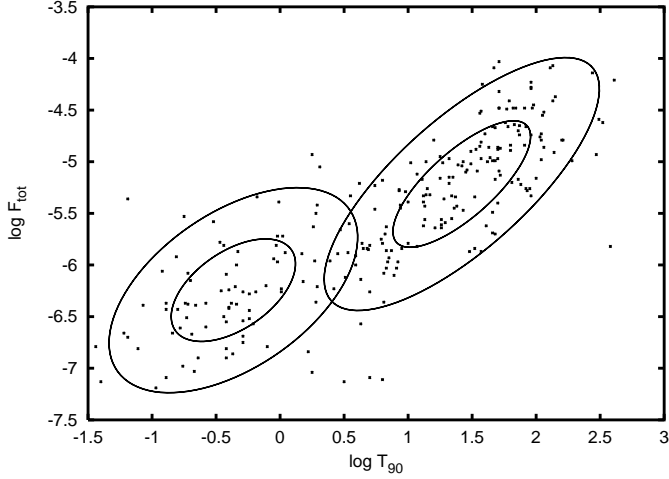
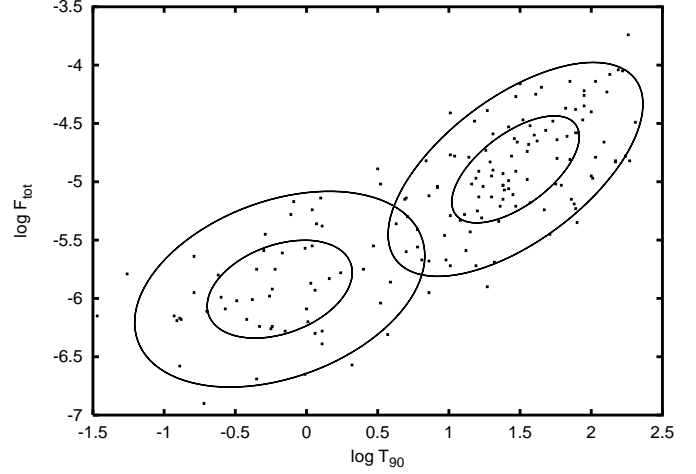
The slopes of short GRBs obtained for the bins No. 7 and No. 8 differ remarkably from those in bins No. 4–6. They are based, however, on a small number of bursts; hence, the r parameter is highly uncertain. Since we used for weighting the number of GRBs within the given bin their, contribution to the final result is marginal. We noted above that the duration and peak flux are independent stochastic variables. Since the sample was splitted into subsamples by the peak flux, this means that the parameters of Gaussians distributions referring to T_{90} either in the Table 2 or in Table 3 should be identical within the statistical uncertainty of estimation. Inspecting a_x in these tables – which summarize the results of the EM algorithm – clearly demonstrates that their difference is much less than σ_x . It is also possible to compare the mean slopes obtained by weighting the results for the short and long GRBs, respectively, in order to test the significance of the difference between these groups. One may compute a $\chi^2 = (m_1 - m)^2 / \sigma_1^2 + (m_2 - m)^2 / \sigma_2^2$

Table 2. Results of the ML fitting for the short GRBs using the EM algorithm. Weighted mean for m is $m = 0.81 \pm 0.06$.

Strip No.	rel. frequency	a_x	a_y	σ_x	σ_y	r	total No. of GRBs	$m = \tan \alpha$
4.	.293	-.199	-6.587	.549	.502	.593	434	0.86
5.	.418	-.275	-6.488	.575	.503	.591	365	0.80
6.	.321	-.365	-6.244	.486	.497	.515	254	1.04
7.	.332	-.188	-5.921	.510	.420	.342	166	0.58
8.	.358	-.325	-5.910	.440	.347	.279	95	0.46

Table 3. Results of the ML fitting for the long GRBs using the EM algorithm. Weighted mean for m is $m = 1.11 \pm 0.03$.

Strip No.	rel. frequency	a_x	a_y	σ_x	σ_y	r	total No. of GRBs	$m = \tan \alpha$
4.	.707	1.560	-5.485	.400	.434	.586	434	1.15
5.	.582	1.613	-5.239	.445	.463	.599	365	1.07
6.	.679	1.419	-5.216	.538	.613	.753	254	1.19
7.	.668	1.468	-4.894	.448	.459	.610	166	1.04
8.	.642	1.391	-4.779	.541	.531	.656	95	0.97

**Fig. 3.** The best ML fits of the two log-Gaussian distributions for the sample No. 6 with $N = 254$.**Fig. 4.** The best ML fits of the two log-Gaussian distributions for the sample No. 7 with $N = 166$.

variable based on the assumption that the m_1, m_2 slopes of the short and long GRBs differs from the m weighted mean only by chance. Making this assumption one obtains $\chi^2 = 22.2$ indicating that the null hypothesis, i.e. $m_1 = m_2$, should be rejected on a 4.7σ significance level. *The two slopes are different.*

4.4. Possible sources of the biases

The relationships derived in the previous subsection refer to the observed values of GRBs. There is a dilemma, however, how representative they are for the true quantities of GRBs not affected by the process of detection. We mentioned already several major source of bias. Here we summarize them again:

- Some GRBs below the threshold remain undetected. Therefore, the stochastic properties of the observed part of the true joint distribution of $\{\log T_{90}, \log F_{\text{tot}}\}$ are not necessarily relevant for the whole population.

- Observed duration refers to the detected part of GRBs. The real duration might be much longer.
- There is a similar bias also for the fluence.
- Additionally, due to the limited spectral response of BATSE, a significant fraction of the high energy part of the fluence may remain unobserved.
- There is a special bias at short GRBs. At GRB, where the duration is shorter than the time resolution of detection, there is a one-to-one correspondence between the peak flux and the fluence.

4.4.1. Effect of the threshold

Using the law of full probability we decomposed the observed joint probability distribution of $\{\log T_{90}, \log F_{\text{tot}}\}$ into the distribution of the peak flux and a conditional probability, assuming p is given. Since the detection proceeds on three different time scales, one does not expect a sharp cut on $G(p)$ but the

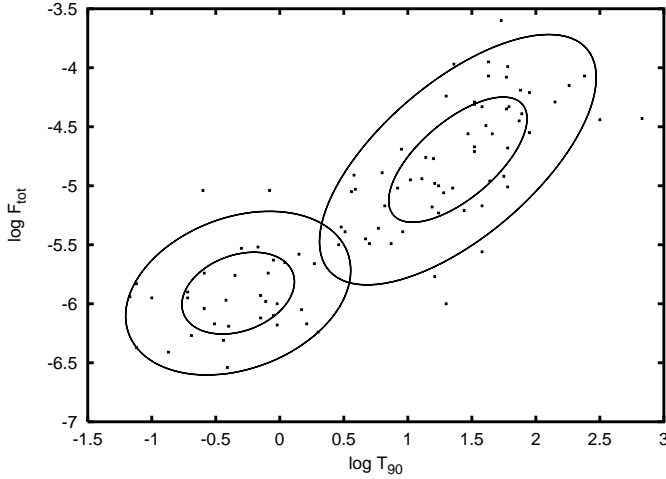


Fig. 5. The best ML fits of the two log-Gaussian distributions for the brightest sample No. 8 with $N = 95$.

distortion is more complicated in the reality. Although the observational threshold may seriously affect the detected form of $G(p)$, it need not necessarily modify $P(F_{\text{tot}}, T_{90}|p)$. The detection threshold, however, may distort also the fluence and duration themselves, and in this way also the form of $P(F_{\text{tot}}, T_{90}|p)$.

4.4.2. True vs. observed duration

Depending on the light curve of the GRBs a significant fraction of the outbursts may remain unobserved. So the duration derived from the observed part is only a lower limit for the true one. Approaching the detection threshold this effect should become more and more serious. Assuming a Gaussian form for $P(F_{\text{tot}}, T_{90}|p)$ one expect a systematic change in the parameters as one is approaching the threshold. Inspecting the mean values and standard deviations of the duration in the tables of the Appendix, one may really recognize this effect in the three faintest bins. In the remaining part of the sample, however, there is a remarkable homogeneity in the mean value and standard deviation of duration. It is also worth mentioning that the same is true in Tables 2 and 3 summarizing the result of the ML fitting. So one may conclude that this bias does not play a significant influence in the 4–8. bins used for our calculations.

4.4.3. True vs. observed fluence

Similarly to the duration also the observed fluence might be a lower bound depending on the light curve of the burst. Although fixing p resulted in a similar functional (Gaussian) form of the fluence as of the duration, its mean value a_y differs from bin to bin due to the dependence of F_{tot} on the peak flux. Its standard deviation σ_y , however, shows a noticeable homogeneity within the limits of statistical uncertainty. Again, this implies a constancy in the functional form of $P(F_{\text{tot}}, T_{90}|p)$ in the bins studied. The only exception is perhaps the bin No. 8 for the short GRBs, where the standard deviation and the r correlations coefficient seems to depart considerably from the others in Table 2. One may test the significance of the excursion of σ_y in bin No. 8 by performing a F test (see e.g.

Kendall & Stuart 1976). Computing the $F = \sigma_8^2/\sigma_5^2$ value, where the indexes refer to the serial number of bins, one obtains $F = 2.11$ indicating significant difference on the 99.9% level. Except for this significant excursion in the 8th bin, the σ_y values are statistically identical implying that the functional relationship between F_{tot} and T_{90} is not significantly influenced by the process of detection in the bins studied.

4.4.4. Bias from the spectral response

BATSE were observing in four energy channels. Even the highest energy channel was not able to detect the hardest parts of the bursts. A significant fraction of the incoming energy might remain unobserved. In principle, there is a possibility for estimating the amount of unobserved part of radiation by supposing a spectral model for the GRB. Fitting this model to the values measured in the four energy channels one may get an estimate for the unobserved part. Supposing, the energy distribution of the bursts can be described by two power laws separated by an E_p energy Lloyd & Petrosian 1999 did a four parameter fit (two powers, E_p and an amplitude) for GRBs detected by BATSE. A basic trouble at this approach appears in the fact that numbers of points and parameters to be fitted are identical and, consequently, any uncertainty in the measured values has a very sensitive impact on the parameters estimated. Moreover, a significant fraction of GRBs does not have a reliable fluence in the high energy channel which exceeds at least the 3σ level of the background. In particular, it is true for the No. 4–8. bins.

It is well-known that the short bursts are harder in the average than the long ones. Consequently, the fraction of the unobserved part of the energy spectrum may have a negative correlation with the duration in the case of this subgroup. The detected part of the fluence experiences therefore a positive correlation, assuming there is no intrinsic relationship between the duration and the true total fluence. In the case of a real intrinsic relationship between these quantities, the apparent correlation from the spectral bias may have a contribution to the real one. One may expect that the spectral bias is more serious at bursts, where the whole high energy fluence is buried into the background noise. So one expect a gradual change in the slope of the relationship between F_{tot} , and T_{90} as one proceeds from the faint bursts to the brighter ones. Tables 4 and 5 summarize the frequency of bursts having different S/N (“signal-to-noise”) ratios within the studied peak flux bins, separately.

It is clear from Table 5 that the long faint bins are dominated by bursts with no significant high energy fluence. The contrary is true for the brighter ones. Proceeding from the faint burst to the bright ones one does not see a gradual change in the slope of the $\{\log F_{\text{tot}}, \log T_{90}\}$ relationship. Hence, we may conclude that the spectral bias makes only a marginal contribution, and the correlation observed is close to the real one. For the short bursts (Table 4), in the contrary, a significant change is observed, which might be interpreted as a clear sign of spectral bias. It implies, furthermore, that the real slope, if any, is smaller than the observed one. This fact strengthens the conclusion on the difference between the short and long GRBs with respect of the $\{\log F_{\text{tot}}, \log T_{90}\}$ relationship.

Table 4. Frequency of S/N ratios of fluences in the high energy channel for GRBs of $T_{90} < 2$ s (the integer numbers given in the header are the truncated S/N values).

Bin	S/N				Row Total
	.00	1.00	2.00	>3.00	
1.	0	1	0	0	1
2.	3	0	1	1	5
3.	19	10	7	8	44
4.	57	15	14	18	104
5.	53	28	14	31	126
6.	17	16	17	29	79
7.	4	3	4	36	47
8.	2	4	4	24	34
9.	0	0	3	19	22
10.	1	0	1	4	6
11.	0	0	0	5	5
12.	0	0	0	2	2
13.	0	0	0	1	1
Column	156	77	65	178	476
Total	32.8	16.2	13.7	37.4	100.0%

Table 5. Frequency of S/N ratios of fluences in the high energy channel for GRBs of $T_{90} > 2$ s (the integer numbers given in the header have the same meaning as in Table 4).

Bin	S/N				Row Total
	.00	1.00	2.00	>3.00	
1.	2	1	0	1	4
2.	71	19	7	11	108
3.	193	58	37	53	341
4.	135	65	42	88	330
5.	72	33	40	94	239
6.	33	23	16	103	175
7.	12	9	10	88	119
8.	1	2	7	51	61
9.	1	1	1	49	52
10.	0	0	0	33	33
11.	0	0	0	14	14
12.	0	0	0	13	13
13.	0	0	0	5	5
14.	0	0	0	2	2
Column	520	211	160	605	1496
Total	34.8	14.1	10.7	40.4	100.0%

4.4.5. Bias from the finite time resolution

We mentioned above the detection proceeded on three (64 ms, 256 ms and 1024 ms) time scales. The incoming photons were binned in these time scales and the bin having the maximum count rate were used for triggering the detection. The bursts having $T_{90} < 64$ ms, however, consist of only one bin, consequently, the fluence and the peak flux are based on the same incoming photons on this time scale. If the incoming photons of a burst had the same energy fixing p would mean fixing F_{tot} as well and equation (4) is no longer valid since T_{90} does not have any impact on the fluence observed. By fixing p this effect degenerate the distribution of F_{tot} into one point and it does no longer reflects the distribution of T_{90} we supposed. In the

Table 6. Mean values and standard deviations of the total fluences and the 64 ms peak fluxes within the first ten 64 ms bin of the T_{90} duration. Except the fluence in the first bin all the values do not differ from those of the entire sample, within the limits of statistical uncertainties.

Bin	$\log F_{\text{tot}}$		$\log p_{64}$		corr. coeff.	no. of GRBs
	mean	st. dev.	mean	st. dev.		
1.	-7.0243	.5043	.3535	.1912	.7625	17
2.	-6.6280	.5109	.3815	.2447	.6333	33
3.	-6.6756	.5122	.3690	.2379	.6335	37
4.	-6.4863	.5408	.4090	.2629	.5793	36
5.	-6.5480	.4428	.3691	.2460	.7125	26
6.	-6.5804	.5637	.3482	.2370	.6117	16
7.	-6.4492	.3823	.4191	.2278	.2241	31
8.	-6.3312	.4756	.4278	.2802	.6868	20
9.	-6.4532	.4517	.3348	.2382	.6780	16
10.	-6.4292	.3826	.3682	.2258	.5620	16
entire sample	6.5599	.5015	.3828	.2395	.5822	248

reality, however, the energies of the incoming photons have a wide range and this effect is not so pronounced.

As the duration covers an increasing number of bins of 64 ms the particular bin representing the peak flux has a decreasing impact on the value of the fluence. In Table 6 we gave some stochastic parameters (mean, standard deviation, correlation) of the joint distribution of $\log F_{\text{tot}}$ and $\log p_{64}$ within the first 10 bins of T_{90} of 64 ms, in order to see the possible quantitative differences. Except the mean value of $\log F_{\text{tot}}$ in the first bin, which deviate from the sample value at about 1σ level there is no striking differences between the parameters. For testing the possible differences between the bins in Table 6 we did a multivariate analysis of variance (MANOVA) which compares the variances and covariances of variables within the bins and between them. The analysis resulted in a difference on the 99.5% significance level. The MANOVA module of the SPSS software package was used for these calculations². Repeating the calculation but abandoning the first bin, the suspected outlier, the significance dropped back to 50.4% inferring that the distributions in bins 2–10. were identical within the limits of statistical uncertainty. Even if we treated the excursion of the bin No. 1 as a real effect there is only a small number of GRBs in it (see Table 1) which do not affect the final results in Tables 2 and 3.

Summing up the discussions we performed in this subsection on the different bias we may conclude that either they do not have a significant impact on the final result (i.e. there is a significant difference in the $\{\log F_{\text{tot}}, \log T_{90}\}$ correlation between the short and long GRBs) or the observed difference in the relationship is even enhanced in the reality if we considered the bias properly.

5. Discussion

We have presented evidence indicating that there is a power-law relationship between the logarithmic fluences and the

² SPSS is a registered trademark. See SPSS home page in references.

logarithmic T_{90} durations of the GRBs in the Current BATSE Catalog, based on the EM maximum likelihood estimation of the parameters of the bivariate distribution of these measured quantities. This relationship holds for both subclasses of GRBs separately. As shown in the Appendix, the dispersions of the T_{90} do not differ significantly from those of the T_{50} distributions, and therefore the same correlations and the same power-law relations would be expected if one used the T_{50} instead of the T_{90} . We have also evaluated the possible impact of instrumental biases, with the results that the conclusions do not change significantly when these effects are taken into account.

An intriguing corollary of these results is that the exponents in the power-law dependence between the fluence and the duration differs significantly for the two groups of short ($T_{90} < 2$ s) and long ($T_{90} > 2$ s) bursts at a 4.7σ level. As shown in Sect. 4.4, this also means that the same power law relations hold between the total energy emitted (E_{tot}) and the intrinsic durations (t_{90}) of the two groups. The intrinsic nature of this relation is also confirmed by further calculations based on a principal component analysis.

While an understanding of such power-law relations in terms of physical models of GRB would require more elaborate considerations, we note that there is substantial evidence indicating the two classes of bursts are physically different. First, there is the fact that short bursts are harder (Kouveliotou et al. 1993); this is confirmed also by the analysis of Mukherjee et al. (1998). Then, there is evidence that the spectral break energies of short bursts are larger than for long bursts (Paciesas et al. 2001). The short bursts have a different spectral lag vs. luminosity ratios than long bursts (Norris et al. 2001). Finally, the number of sub-pulses, and the soft-to-hard evolution is different depending on the duration (Gupta et al. 2002).

The results obtained here are compatible with a simple interpretation where the bursts involve a wind outflow leading to internal shocks responsible for the gamma-rays (Rees & Mészáros 1994; Piran 1999), in which the luminosity is approximately constant over the duration t of the outflow, so that both the total energy E_{tot} and the fluence F_{tot} are $\propto t$. If an external shock were involved, (e.g. Mészáros & Rees 1993; Piran 1999), for a sufficiently short intrinsic duration (impulsive approximation) there would be a simple relationship between the observed duration and the total energy, $t \propto E^{1/3}$, resulting from the self-similar behavior of the explosion and the time delay of the pulse arrival from over the width of the blast wave from across the light cone. This relationship is steeper than the one we deduced for long bursts.

The fluence – duration relation of GRBs which we have discussed here appears to be physical, and it is significantly different for the short and the long bursts. For the short ones, the total energy released is proportional to the $m = 0.81$ power of duration of the gamma ray emission, while for the long ones it is proportional roughly to the of $m = 1.11$ power of the duration. This may indicate that two different types of central engines are at work, or perhaps two different types of progenitor systems are involved. It is often argued that those bursts for which X-ray, optical and radio afterglows have been found, all of which belong to the long-duration group, may be due to the collapse of a massive stellar progenitor (e.g. Paczyński 1998;

Fryer et al. 1999). The short bursts, none of which have as of August 2002 yielded afterglows, may be hypothetically associated with neutron star mergers (e.g. Fryer et al. 1999) or perhaps other systems. While the nature of the progenitors remains so far indeterminate, our results provide new evidence suggesting an intrinsic difference between the long and short bursts, which probably reflects a difference in the physical character of the energy release process. This result is completely model-independent, and if confirmed, it would provide a potentially useful constraint on the types of models used to describe the two groups of bursts.

6. Conclusions

In summary, we have presented quantitative arguments in supporting two new results, namely that there is a power law relation between the fluence and duration of GRBs which appears to be physical, and that this relation is significantly different for the two groups of short and long bursts. In addition, estimations of the concrete values of exponents were obtained, two. For the short subgroup one obtains $m \approx (0.46-1.04)$ with the most probable value around $m \approx 0.81$. (In the reality, however, this value could be much smaller due to a possible strong spectral bias). For the long subgroup one obtains $m \approx (0.97-1.19)$ with the most probable value around $m \approx 1.11$. The difference is significant on the 4.7σ level.

For the short ones, the total energy released is weakly depending on the duration of the gamma ray emission, while for the long ones it is proportional roughly to the duration. While the nature of the progenitors remains so far indeterminate, our results provide new evidence suggesting an intrinsic difference between the long and short bursts, which probably reflects a difference in the physical character of the energy release process. This result is completely model-independent, and if confirmed, it would provide a potentially useful constraint on the types of models used to describe the two groups of bursts.

These results were obtained exclusively from the statistical studies of BATSE data (using the known redshifts of the observed afterglows, too) applying only the mathematical Cramér theorem and the law of full probability, respectively. It is highly surprising that these pure mathematical theorems allowed to obtain these remarkable results.

Acknowledgements. We are indebted to Dr. Gábor Tusnányi (Rényi Institute for Mathematics), Dr. Chryssa Kouveliotou and Dr. Michael Briggs (NASA MSFC) for useful discussions and critique. We are indebted to an anonymous referee for the valuable remarks. This research was supported in part through OTKA grants T024027 (L.G.B.), F029461 (I.H.) and T034549, NASA grant NAG-9192 and NAG-9153, (P.M.), and Czech Research Grant J13/98: 113200004 (A.M.).

Appendix A: Comparison of T_{90} and T_{50} statistical properties

In order to check, whether there is some influence of the time dilatation on the distribution of T_{90} or T_{50} , we compare here the basic properties of these two quantities in our sample for the long and the short bursts, separately. We grouped the data,

Table A.1. GRBs of long duration ($T_{90} > 2$ s).

$\log P_{256}$	$\log T_{90}$	$\log T_{50}$	$\sigma_{\log T_{90}}$	$\sigma_{\log T_{50}}$	No. of GRBs
-.50	1.24	.85	.48	.47	49
-.30	1.42	1.00	.47	.50	230
-.10	1.48	1.08	.49	.53	309
.10	1.46	1.02	.51	.57	272
.30	1.51	1.01	.52	.61	194
.50	1.43	.94	.51	.59	161
.70	1.45	.96	.48	.56	104
.90	1.42	.83	.54	.62	56
1.10	1.41	.83	.50	.49	44
1.30	1.44	.88	.50	.53	34
>1.40	1.21	.68	.41	.50	29

Table A.2. GRBs of short duration ($T_{90} < 2$ s).

$\log P_{256}$	$\log T_{90}$	$\log T_{50}$	$\sigma_{\log T_{90}}$	$\sigma_{\log T_{50}}$	No. of GRBs
-.50	-.57	-.87	.55	.60	7
-.30	-.65	-1.01	.53	.57	43
-.10	-.40	-.77	.49	.51	103
.10	-.35	-.74	.35	.32	105
.30	-.33	-.75	.39	.41	75
.50	-.27	-.69	.35	.36	54
.70	-.29	-.72	.36	.34	25
.90	-.35	-.76	.39	.36	22
1.10	-.18	-.72	.44	.39	7
1.30	-.74	-1.21	.31	.43	5
>1.40	-.72	-.90	.00	.00	1

using the 256 ms peak flux values, into 0.2 bins in P_{256} , and summarized in Tables A.1 and A.2 the mean values and the corresponding standard deviations of the logarithmic durations of GRBs in each peak flux bin. We stress that this does not include any equalization of the noise level in the various bins, and is not intended as a test of the time dilatation hypothesis, but rather as a test of whether dilatation would have any effect on our results. Inspecting the durations of long ($T_{90} > 2$ s) GRBs summarized in Table A.1 one sees that, except from the brightest and faintest bins, there is no significant difference in $\log T_{90}$. The decrease of the duration in the faintest bin is probably due to the biasing of the determination, namely, the fainter parts of the bursts cannot be discriminated against the background, and therefore the duration obtained is systematically shorter. There is a remarkable homogeneity and no trend in the standard deviations of the $\log T_{90}$. In the case of the long burst T_{50} durations, this quantity shows an increasing trend towards the bursts of fainter peak flux. The shortening in the faintest bin is probably also due to selection effects. Similarly to the $\log T_{90}$ values, the same homogeneity can be observed in the standard deviations also in case of $\log T_{50}$. The standard deviations are almost the same in both $\log T_{90}$ and $\log T_{50}$. One can test whether, within our analysis methodology and with our sample, there is a significant difference among the binned T_{90} values, and whether the slight trend in the T_{50} significantly differs from zero. To evaluate the significance of these data we performed a

one way analysis of variance with the ANOVA program from a standard SPSS package. The ANOVA compares the variances within sub-samples of the data (in our case within bins), with the variances between the sub-samples (bins).

In the case of $\log T_{90}$ the probability that the difference is accidental is 66%. In the case of the T_{50} durations the same quantities (variances within and between bins) gives a probability of 98.5% for being a real difference between bins, or a probability of 1.5% that there is no difference between the bins. This figure gives some significance for the reality of a trend in the data; however, this value of 0.2 explains less than 1/6 of the variance of T_{50} within one bin. We may conclude that even in this case the variance is mainly intrinsic.

Inspecting the same data in the case of the short duration bursts (Table A.2) we come to a similar conclusion, i.e. there is no sign of trends in the durations of the different bins. Dropping the two faintest bins, which are definitely affected by biases, and dropping the poorly populated brightest bins, we arrive by the analysis of variances with ANOVA to probabilities of 53% and 92.1% for the difference being purely accidental between bins in T_{90} and T_{50} , respectively.

References

- Bagoly, Z., Mészáros, A., Horváth, I., et al. 1998, ApJ, 498, 342
- Balastegui, A., Ruiz-Lapuente, P., & Canal, R. 2001, MNRAS, 328, 283
- Cramér, H. 1937, Random variables and probability distributions, Cambridge Tracts in Mathematics and Mathematical Physics, No. 36 (Cambridge: Cambridge University Press)
- Dempster, A. P., Laird, N. M., & Rubin, D. R. 1977, J. Roy. Stat. Soc. B, 39, 1
- Efron, B., & Petrosian, V. 1992, ApJ, 339, 345
- Fenimore, E. E., & Bloom, J. S. 1995, ApJ, 453, 16
- Fryer, C. L., Woosley, S. E., & Hartmann, D. H. 1999, ApJ, 526, 152
- Greiner, J. 2002, <http://www.aip.de/~jcg/grbgen.html>
- Gupta, V., Das Gupta, P., & Bhat, P. N. 2002 [astro-ph/0206402]
- Hakkila, J., Haglin, D. J., Roiger, R. J., et al. 2000a, in Gamma-Ray Bursts; 5th Huntsville Symp., ed. R. M. Kippen, R. S. Mallozzi, & G. J. Fishman (Melville: AIP), 33
- Hakkila, J., Meegan, C. A., Pendleton, G. N., et al. 2000b, in Gamma-Ray Bursts; 5th Huntsville Symp., ed. R. M. Kippen, R. S. Mallozzi, & G. J. Fishman (Melville: AIP), 48
- Hakkila, J., et al. 2000c, ApJ, 538, 165
- Horváth, I. 1998, ApJ, 508, 757
- Horváth, I. 2002, A&A, 392, 791
- Horváth, I., Mészáros, P., & Mészáros, A. 1996, ApJ, 470, 56
- Kendall, M., & Stuart, A. 1976, The Advanced Theory of Statistics (Griffin, London)
- Kouveliotou, C., Meegan, C. A., Fishman, G. J., et al. 1993, ApJ, 413, L101
- Lamb, D. Q., Graziani, C., & Smith, I. A. 1993, ApJ, 413, L11
- Lee, T., & Petrosian, V. 1996, ApJ, 470, 479
- Lee, T., & Petrosian, V. 1997, ApJ, 474, L37
- Litvin, V. F., Matveev, S. A., Mamedov, et al. 2001, Pis'ma v Astronomicheskii Zhurnal, 27, 495
- Lloyd, N. L., & Petrosian, V. 1999, ApJ, 511, 550
- McBreen, S., Quilligan, F., McBreen, B., et al. 2001, AA, 380, L31
- Meegan, C. A., Pendleton, G. N., Briggs, M. S., et al. 1996, ApJS, 106, 65 (3B BATSE Catalog)

- Meegan, C. A., Pendleton, G. N., Briggs, M. S., et al. 2001, Current BATSE Gamma-Ray Burst Catalog <http://gamma-ray.msfc.nasa.gov/batse/grb/catalog/current/>
- Meegan, C. A., Hakkila, J., Johnson, A., et al. 2000, in Gamma-Ray Bursts; 5th Huntsville Symp., ed. R. M. Kippen, R. S. Mallozzi, & G. J. Fishman (Melville: AIP), 43
- Mészáros, A., & Mészáros, P. 1996, ApJ, 466, 29
- Mészáros, A., Bagoly, Z., & Vavrek, R. 2000a, A&A, 354, 1
- Mészáros, A., Bagoly, Z., Horváth, I., et al. 2000b, ApJ, 539, 98
- Mészáros, P., & Mészáros, A. 1995, ApJ, 449, 9
- Mészáros, P., & Rees, M. J. 1993, ApJ, 405, 278
- Mukherjee, S., Feigelson, E. D., Jogesh Babu, G., et al. 1998, ApJ, 508, 314
- Norris, J. P., Nemiroff, R. J., Scargle, J. D., et al. 1994, ApJ, 424, 540
- Norris, J. P., Bonnell, J. T., Nemiroff, R. J., et al. 1995, ApJ, 439, 542
- Norris, J. P., Scargle, J. D., & Bonnell, J. T. 2001, in Gamma-Ray Bursts in the Afterglow Era, Proc. of the Intern. Workshop, Rome, Italy, 17-20 Oct. 2000, ed. E. Costa et al. (Springer), 40
- Quilligan, F., McBreen, B., Hanlon, L., et al. 2002, AA, 385, 377
- Paciesas, W. S., Meegan, C. A., Pendleton, G. N., et al. 1999, ApJS, 122, 465 (4B BATSE Catalog)
- Paciesas, W. S., Preece, R. D., Briggs, M. S., et al. 2001, in Gamma-Ray Bursts in the Afterglow Era, Proc. of the Intern. Workshop, Rome, Italy, 17-20 Oct. 2000, ed. E. Costa et al. (Springer), 13
- Paczyński, B. 1998, ApJ, 497, L45
- Peebles, P. J. E. 1993, Principles of Physical Cosmology (Princeton: Princeton University Press)
- Pendleton, C. N. 1997, ApJ, 489, 175
- Petrosian, V., & Lee, T. 1996, ApJ, 467, L29
- Piran, T. 1999, Phys. Rep., 314, 575
- Press, W. H., Flannery, B. P., Teukolsky, S. A., et al. 1992, Numerical Recipes (Cambridge: Cambridge University Press)
- Rees, M. J., & Mészáros, P. 1994, ApJ, 430, L93
- Reichart, D. E., & Mészáros, P. 1997, ApJ, 483, 597
- Rényi, A. 1962, Wahrscheinlichkeitsrechnung (Berlin: VEB Deutscher Verlag der Wissenschaften)
- SPSS Inc., <http://www.SPSS.com>
- Stern, B., Poutanen, J., & Svensson, R. 1999, ApJ, 510, 312
- Trumpler, R. J., & Weaver, H. F. 1953, Statistical Astronomy (Berkeley: University of California Press)
- Ulmer, A., & Wijers, R. A. M. J. 1995, ApJ, 439, 303
- Weinberg, S. 1972, Gravitation and Cosmology (New York: Wiley)
- Wijers, R. A. M. J., & Paczyński, B. 1994, ApJ, 437, L107